PROCEEDINGS OF SPIE

SPIEDigitalLibrary.org/conference-proceedings-of-spie

Performance of the facility instruments on the Hobby-Eberly telescope

Hill, Gary, MacQueen, Phillip, Ramsey, Lawrence

Gary J. Hill, Phillip J. MacQueen, Lawrence W. Ramsey, "Performance of the facility instruments on the Hobby-Eberly telescope," Proc. SPIE 4841, Instrument Design and Performance for Optical/Infrared Ground-based Telescopes, (7 March 2003); doi: 10.1117/12.461901

SPIE.

Event: Astronomical Telescopes and Instrumentation, 2002, Waikoloa, Hawai'i, United States

Downloaded From: https://www.spiedigitallibrary.org/conference-proceedings-of-spie on 15 Jul 2020 Terms of Use: https://www.spiedigitallibrary.org/terms-of-use

Performance of the facility instruments on the Hobby-Eberly Telescope*

Gary. J. Hill†, Phillip J. MacQueen,

McDonald Observatory, University of Texas at Austin, RLM 15.308, Austin, TX 78712, USA

& Lawrence W. Ramsey

Department of Astronomy and Astrophysics, Pennsylvania State University, University Park, PA 16802, USA

ABSTRACT

The Hobby-Eberly Telescope (HET) is a revolutionary large telescope of 9.2 meter aperture, located in West Texas at McDonald Observatory. Early scientific operations started on October 8, 1999. The HET operates with a fixed segmented primary and has a tracker which moves the four-mirror corrector and prime focus instrument package to track the sidereal and non-sidereal motions of objects. As of two years ago, the HET was taking science data but the image quality and primary mirror stability were far from specifications. We established the HET Completion Project to identify and fix these problems, and here we describe the current performance of the HET relative to its goals, focusing on progress made in the past two years.

The first phase of HET instrumentation includes three facility instruments: the Low Resolution Spectrograph (LRS) and High Resolution Spectrograph (HRS), which are in operation, and the Medium Resolution Spectrograph (MRS), which will be commissioned in the summer and autumn. The current status of the instruments is described in detail with performance measures.

Keywords: Telescopes: Hobby-Eberly Telescope, Astronomical instrumentation: Spectrographs

1. INTRODUCTION: OVERVIEW OF THE HET AND INSTRUMENTS

The HET[1,2] is a unique telescope with an 11 m hexagonal-shaped spherical mirror made of 91 1 m Zerodur™ hexagonal segments that sits at a fixed zenith angle of 35°. It can be moved in azimuth to access about 70% of the sky visible at McDonald Observatory. HET is a collaboration of the University of Texas at Austin, Pennsylvania State University, Stanford University, Georg-August-Universität, Göttingen, and Ludwig-Maximillians-Universität, Munich. The pupil is 9.2 m in diameter, and sweeps over the primary as the x-y tracker follows objects for between 40 minutes (in the south at $\delta = -10.3^{o}$) and 2.8 hours (in the north at $\delta = +71.6^{o}$). The maximum track time per night is 5 hours and occurs at $+63^{o}$. Detailed descriptions of the HET and its commissioning can be found in refs 1-5. Currently the HET is operating with its first two facility instruments, the Marcario Low resolution Spectrograph (LRS)[6-8], which rides in the Prime Focus Instrument Package (PFIP) on the tracker, allowing it to image as well as take spectra, and the fiber-fed High Resolution Spectrograph (HRS)[9] installed in the basement spectrograph room under the telescope internal to the pier. The Medium Resolution Spectrograph (MRS)[10,11] is being assembled in the spectrograph room, and is expected to enter commissioning later this year. The HRS and MRS are fed by fibers from the fiber instrument feed (FIF) [10] that is part of the PFIP.

The primary mirror has a radius of curvature of 26164 mm, and a 4-mirror double-Gregorian type corrector is designed to produce images with FWHM < 0.6 arcsec in the absence of seeing, over a 4 arcmin (50 mm) diameter science field of view[8,12]. A moving baffle is installed at a pupil on the fourth mirror of the corrector and will block stray light as the pupil tracks off the primary. It is undergoing commissioning, currently. Another mirror folds the light-path towards the LRS, for a total of six reflections to reach the LRS slit. The FIF is fed directly without a further reflection.

---

* The Hobby – Eberly Telescope is operated by McDonald Observatory on behalf of the University of Texas at Austin, the Pennsylvania State University, Stanford University, Ludwig-Maximillians-Universität München,and Georg-August-Universität, Göttingen

† G.J.H.: E-mail: hill@astro.as.utexas.edu

Instrument Design and Performance for Optical/Infrared Ground-based Telescopes,
Masanori Iye, Alan F. M. Moorwood, Editors, Proceedings of SPIE Vol. 4841 (2003)
© 2003 SPIE · 0277-786X/03/$15.00

Downloaded From: https://www.spiedigitallibrary.org/conference-proceedings-of-spie on 15 Jul 2020
Terms of Use: https://www.spiedigitallibrary.org/terms-of-use

The HET optics are silver-coated (Denton Vacuum FS99™ enhanced silver) and the throughput (with 6 reflections to reach the LRS) drops rapidly below 400 nm (see below). The first HET instruments are hence principally designed for the wavelength region between 400 and 1000 nm. However, a number of science projects would benefit from coverage down to 370 nm (to include the [OII] λ3727 line, for example), and the LRS is the only HET facility instrument able to work that blue.

2. HET CURRENT PERFORMANCE

The HET is a prototype for a new breed of cost-effective large telescopes. As such, it is essentially a test-bed for engineering and operations concepts designed to minimize cost while maintaining performance. In particular, the primary mirror[13], based on a steel truss, and the star tracker[14] were key to realizing the project for the initial modest cost of $16M. Initial performance of the HET was not, however, to specification in the areas of image quality and primary mirror stability[2]. Subsequent completion of the telescope to improve image quality as described below, will bring the total expenditure to about $20M, still a very modest price for a large telescope. Here we describe the current performance compared to specifications, and look forward to the realization of full performance.

In conjunction with image quality improvements at HET, we now have a one-year baseline of site seeing measurements recorded by Direct Image Motion Monitors[15]. The median zenith seeing has been 1.0 arcsec FWHM with the best images being 0.7 arcsec or better 9% of the time. The summer seeing is better than in winter (0.9 versus 1.3 arcsec). At the 35 degree zenith distance of the HET, this translates to a median of 1.13 arcsec, and minimum of 0.8 arcsec FWHM.

2.1 Image quality improvements

The image quality delivered by the HET depends on (a) the accuracy of the primary mirror alignment (stack), (b) the stability of the primary mirror to changes in temperature and gravity, (c) dome seeing, (d) accuracy of the motions of the tracker, and (e) the figure and internal alignment of the corrector. Two years ago, typical images delivered by the telescope were 2.7 arcsec FWHM [4]. Since then, we have undertaken a series of projects designed to understand the poor image quality of the HET and to correct the problem, with the goal of achieving the HET image quality specification of 0.9 arcsec FWHM in the best expected site-seeing of 0.7 arcsec. At present, the best images recorded (by the LRS in imaging mode) have been 1.2 arcsec FWHM, a huge improvement over the situation a year ago. The median image quality is now 1.5 arcsec FWHM. Here we briefly report the projects that have resulted in this improvement. Refer to ref 2 for full details.

2.1.1 The Mirror Alignment Recovery System (MARS)

The polarizing shearing interferometer system (CCAS) delivered with the HET to effect the alignment (stacking) of the 91 mirror segments to form a single image, proved to be unusable in practice. After a significant evaluation and commissioning effort[16], we determined that the capture range of the CCAS instrument was inadequate. As a replacement, we elected to build a prototype Shack-Hartmann system, to produce an image from each mirror that could be aligned with a fiducial spot. This system, called MARS-I, has been operational since October 2001 and has dramatically improved the quality of the primary mirror alignment. At this point, we are able to align the mirror segments to 0.28 arcsec rms (projected on the sky), and this now has a negligible effect on the delivered image quality. The HET specifications required this value to be 0.12 arcsec rms, but our alignment accuracy is limited by the dome seeing, and we expect them to improve in unison. The prototype system will be replaced by a final system (MARS-II [17]) at the end of the year.

2.1.2 The Segment Alignment Maintainence System (SAMS)

The SAMS project corrects a significant shortfall in the HET primary mirror (PM) stability. We were experiencing significant degradation in the quality of the alignment in typically only 1-2 hours, primarily due to temperature driven motions of the mirror segments on the PM truss. NASA Marshall Space Flight Center and Blueline Engineering were contracted to produce an edge sensor system for the HET PM utilizing small inductive sensors. The project started in November 1999, and is approaching completion. The SAMS has been in operation since January 2002, and has already had a significant positive effect on the image quality and efficiency of operations. For temperature changes within +/-1.5 degrees of the temperature at which the PM was aligned, the degradation of the image size is less than 1.0 arcsec FWHM in quadrature, sufficient to degrade stellar images, noticeably. For larger temperature excursions, we are forced to realign the PM with MARS. In practice, two alignments per night are typically required, so the overhead is within the HET specification that <10% of observing time be used for alignment. The performance of SAMS was specified to maintain figure for the temperature range –10 to +25 Celsius, so the system does not yet reach that specification, and may not[18]. The improvement in the overall performance of the HET from the installation of SAMS has, however, been quite dramatic. Maintaining the global radius of curvature (GROC) of the PM within +/-0.3 mm of 26,164 mm is an important aspect of HET performance. GROC is

Downloaded From: https://www.spiedigitallibrary.org/conference-proceedings-of-spie on 15 Jul 2020
Terms of Use: https://www.spiedigitallibrary.org/terms-of-use

controlled by SAMS through a combination of temperature sensing and mirror-gap sensing. Temperature changes drive the ROC of the steel mirror truss and cause the mean gap size between mirrors to change. Gap size is sensed as a common mode by the SAMS, and corrections are applied to the GROC. We believe that with proper calibration this scheme will work, but currently drift in GROC is an operational difficulty that still has to be overcome.

2.1.3 The Dome Ventilation System (DVS)

Dome seeing is the third major component of the poor image quality delivered by HET. The original concept used a down-draft fan system similar to that on the Keck telescopes to draw ambient air in through the dome aperture. The system proved inadequate to the task of flushing the dome under typical conditions encountered in West Texas. In particular, we could improve the seeing significantly by changing from looking down-wind to looking into the wind, and it became obvious that significant perforations of the HET enclosure would be required to prevent stagnant air conditions. The DVS[19] consists of a series of 15 louver panels modeled after those on the Mayall 4 m at KPNO. The louvers were installed between January and April of 2002, and the image quality was seen to steadily improve over this period. The success of the system can be demonstrated on many nights by simply closing the louvers and watching the seeing degrade to 2.5 arcsec!

2.1.4 Tracking and guiding

The fourth aspect of image quality that is unique to the HET design, is the effect of the tracker position on the image. The HET is a complex opto-mechanical system with no natural axes: everything is time-dependent. A trajectory for the tracker is loaded into the tracker control computer from the telescope control computer. This trajectory controls the x-y position of the tracker, and the six hexapod legs and rotation axis that manipulate the payload. In order to track an object accurately, the tracker payload must be maintained on the focal sphere of the spherical primary mirror, and must be pointed accurately perpendicular to it. The tracker[12] has six axes: x, y, focus (z), tip (θ), tilt (ϕ), rotation (ρ). In order to maintain image quality during a track, the "mount model" needs to accurately maintain the 4-mirror corrector in the PFIP perpendicular to the PM within 25 seconds of arc, and in focus to within 10 μm. The tracker is actively guided in x, y only, and the other axes run open-loop. During a track, the PFIP rotates (up to +/-19.4^o in the north) to maintain a fixed PA on the sky. Over the past two years we have eliminated tracking errors in tip/tilt with rotation and have eliminated a guiding (x,y) drift. The drift was not due to flexure, which is generally negligible with such small variations in ρ, but to a combination of the guide algorithm and the evolving lumpy PSF of the telescope, caused by the de-stack of the primary mirror.

With the markedly improved image quality and stability of the primary mirror we are able to evaluate the quality of the mount-model at a lower level than before. Currently, long tracks are showing marked focus drift that appears to be associated with the use of the SAMS. This is to be expected since the SAMS freezes the shape of the mirror instead of letting it follow the expansion of the steel truss. Hence, as the temperature changes, the structure of the telescope expands/contracts but the primary stays fixed. The magnitude of the focus drift that we are seeing is, however, larger than can be accounted for by simple temperature dependence, and we are investigating the behavior of the GROC of the primary under control of SAMS. The current operational fix for these drifts is to refocus the telescope every 20 minutes during a track.

2.1.5 Figure and internal alignment of the corrector

With the image quality of the HET improving markedly, we are approaching the level where the optics might contribute. The corrector[12] has four reflective elements, first three of which are conics and the last is a general asphere. We have undertaken wavefront testing using a Hartmann mask on the pupil at the last mirror in the corrector. The mask places a small aperture over the image of each mirror segment and images either side of focus then allow the image size to be reconstructed without the effect of seeing. Initial indications are that the corrector may be contributing to ~1 arcsec FWHM images, in the absence of seeing. The three conics had null tests and their figures will not degrade the images. The last mirror in the train did not have a null test and was checked with profilometry with an accuracy of only 1 micron, and it may be contributing to the image size. As the dome seeing is eliminated, we may become limited by the optics, but it is too soon to know. Even with such images from the corrector, the HET will be site seeing limited much of the time.

2.1.6 Current performance and prospects

To summarize, the HET is delivering median images to the LRS of 1.5 arcsec FWHM, with the best images in the 1.2 to 1.3 arcsec range. These images are now dominated by dome seeing, rather than by primary mirror alignment or de-stack. The DVS has had a marked effect on the dome seeing, but more efficient flushing of the dome with ambient air is not the whole solution. There are still significant sources of heat (between 500 and 1000 W) on the tracker itself, primarily from the camera controllers of the acquisition and guide cameras, and there is often a turbulent plume visible in images of the telescope pupil.

Downloaded From: https://www.spiedigitallibrary.org/conference-proceedings-of-spie on 15 Jul 2020
Terms of Use: https://www.spiedigitallibrary.org/terms-of-use

These, along with other heat sources inside and outside the dome will be eliminated (see ref 2 for details), and we expect to drive the dome seeing component down to below intrinsic site seeing levels. The focus drift discussed above is a significant barrier to achieving the goal of site-seeing limited observations on long tracks. Currently, observations of 10-15 minutes produce better data than longer exposures, and we are forced to accept the significant overhead of refocusing the tracker often. An upcoming improvement to the guiding system hardware and software will include focus guiding. In the meantime, we look forward to achieving images in the 1.0 to 1.5 arcsec FWHM range on a routine basis in the next year.

2.2 Throughput of the HET

The HET optical design includes five reflections to reach prime focus (six to reach the LRS). Denton Vacuum FSS-99^{TM} enhanced silver was chosen, which has high reflectivity at wavelengths above 400 nm, and is better than bare aluminum for λ>380 nm. Accounting for central obstruction, the pellicle guider, and the atmosphere, the predicted on-axis efficiency is 54% at 600 nm for prime focus and 52% for the light delivered to the LRS. We have encountered significant degradation of these coatings in practice, and Denton Vacuum has already re-coated the corrector mirrors in mid-2000. The primary mirror segment coatings are still the original ones, and have degraded to ~70% reflectivity at 600 nm, rather than 98%. The reason for the initial degradation is that the blue reflectivity of the coatings was specified too tightly, leading Denton Vacuum to utilize a thinner than normal protective overcoat. This thinner coating met the specifications, but proved not to have the durability of earlier Denton Vacuum FSS-99 coatings. The new coatings on the four corrector mirrors and the folding flat that sends light to the LRS have all degraded significantly over the past year (with values between 85 and 95%). As a result, the on-sky throughput of the HET is now about 30% at the LRS input, and 35% at the fiber-feed. We are currently considering options for re-coating the primary mirror, and will re-coat the corrector and fold flat soon. Alternative options are being considered. In the meantime, the effective aperture of the telescope is 6 to 7 m, compared to the 8 to 9 m effective aperture of the HET design (depending on the track length).

2.3 Future activities

The moving baffle, which blocks stray light from the un-illuminated parts of the pupil as it tracks off the primary mirror, is being commissioned this summer. It is located at the pupil on the fifth mirror in the telescope train. We do see stray light ghosts with even a little moonlight if it enters the dome. Additionally, the moving baffle will help to mimic the pupil illumination more accurately for calibration exposures. Calibrating instruments on 8-m class telescopes is not straight-forward, and the moving pupil of the HET presents particular problems. We are utilizing a white reflective target of eight petals that is inserted at the pupil above M3, much as a mirror cover. Calibrating the HRS and MRS will present different challenges as the current system is too faint to give reasonable integration times. We plan to partially rebuild PFIP in the next year and calibration, acquisition and guiding will be revisited during that project.

3. THE FACILITY INSTRUMENTS

Currently, the HET is making queue-scheduled observations with the Marcario Low Resolution Spectrograph (LRS) and the High Resolution Spectrograph (HRS). The Medium Resolution Spectrograph (MRS) will be commissioned during the summer and autumn. Installation started in May. We concentrate on instrument development that has occurred in the last two years since the previous review[4].

3.1 The Marcario Low Resolution Spectrograph

The LRS[6-8] is a high-throughput grism spectrograph with three modes of operation: imaging, longslit, and multi-object. The field of view of the HET is 4 arcmin in diameter, and the LRS has a 13-slitlet Multi Object Spectroscopy (MOS) unit covering this field. The MOS unit[20] is based on miniature components and is remotely configurable under computer control. It is now available for queue observations. All observing modes are now available in the HET queue. A series of longslits (1.0, 1.5, 2.0, 3.0, and 10.0 arcsec wide) may be selected, each 4-arcmin long. Typically, observations are obtained with the 2.0 arcsec wide slit due to the present imaging performance of the HET. A selection of 12 broad band and blocking filters are carried at any one time, along with two grisms. Additional grisms including two echelles are undergoing commissioning and should be available by the end of the year.

The LRS mounts in a restricted space, as part of the PFIP, which rides on the HET tracker. The principal consequence of the tight space and weight constraints is to limit the range of configurations that may be carried by the LRS at any one time. The HET is queue-scheduled, so the limited configurations are factored into the queue-selection of projects executable on any given night. While it might be desirable to have all components available at any time, the overhead of calibrating a large

Downloaded From: https://www.spiedigitallibrary.org/conference-proceedings-of-spie on 15 Jul 2020
Terms of Use: https://www.spiedigitallibrary.org/terms-of-use

number of possible configurations used on a given night does result in considerable inefficiency. We do not consider this limitation to be a significant drawback given the overall operating philosophy for the HET.

The LRS entered early science operations on October 6, 1999. Over the ensuing period we have made significant gains in improving the operational efficiency of the telescope, and the LRS has undergone one significant over-hall. In mid 2001, we discovered that the compressed air supplying the LRS pneumatics was contaminated with oil. We stripped the instrument down to its components, and replaced all the pneumatics. During the course of this rebuild, we examined and cleaned all the optics. The large triplet lens in the collimator[8] is coupled with Dow Corning Q2-3067 gel couplant, and we have discovered evidence that this gel separates over time and can leak a thin clear oil. The bond between the elements in the triplet is still excellent, showing no signs of separating or of small striations that we have seen in some cases. In future we will treat this compound as semi-liquid, providing sealing to avoid leaking the thinner phase of the material. The next time LRS is stripped down for preventative maintenance, we will reinstall the triplet in the cell, sealing the outer elements around their circumferences with RTV to prevent any leakage. Otherwise, the properties of Q2-3067 are superb, and we will continue to use it as the couplant of choice.

3.1.1 The CCD system

Since the last review, significant improvements have been made to the detector system of the LRS. The CCD is a 3072 x 1024, 15 μm pixel (pxl), Ford Aerospace device fabricated circa 1995, thinned and AR coated by the Steward Observatory CCD lab. It has 4 amplifiers, up to two of which can be run at once. The CCD is called SF1, and is blue-optimized with a platinum flash gate and a 500 Angstrom thick hafnium oxide AR coating. The peak RQE is 96% at 450 nm. A de-bonding incident[4] destroyed 3 of the 4 amplifiers, but it has provided excellent data to date. We have recently received a second CCD (SF3) of the same format from the Steward Observatory CCD lab. which has four amplifiers and good cosmetics. This CCD will be held as a spare until demand for high-speed readout is ascertained, at which point we will entertain a swap with the present CCD.

The principal improvements in performance have come from the implementation of the McDonald Observatory Version 2 CCD controller. Details of the controller will be given elsewhere, so we summarize the performance obtained with the SF1 CCD, running one amplifier. The controller can run any two amplifiers at once. The new controller allows readout speeds of 25, 50, and 100 kpxl/s per amplifier at the same gain. The readout noise at 25 kpxl s^{-1} is 5.10 electrons (35.6 seconds readout time, binned 2x2), compared to 5.5 electrons readout noise at 19.2 kpxl s^{-1} (46 seconds readout time, binned 2x2) with the Version 1 controller. Not only is this the best performance we are aware of with this type of CCD, but the fastest mode has had a marked effect on the setup-time overhead for LRS observations. The LRS as an imager is used for acquisition, and much of the overhead was associated with the long readout time of the previous controller. The approximately 1k x 1k square region covered by the 4 arcmin diameter HET field of view can be read out in 3.6 seconds with 6.2 electrons read noise (binned 2x2 at 100 kpxl s^{-1}), and we have reduced the overhead for setup (including telescope move) to about 10 minutes, typically. It often took in excess of 15 minutes before.

In ref 4 we reported our initial experiences with setting up the standard model CryoTiger (CT) cryocooler system with PT-14 gas, manufactured by APD Cryogenics, for the LRS detector in the remote location of the LRS. At that time we had the CT compressor located on a platform mounted on the top member of the top hexagon of the HET structure, and used 75 foot lines to run the cryocooler cold end. Imaging of the HET pupil showed that the 500 W heat output from the compressor was sometimes responsible for seeing degradation, so a year ago we relocated the compressor in the (soon to be) chilled enclosure under the primary mirror, extending the line length to 200 feet. This is well in excess of the 50 foot maximum recommended by APD, but initial concerns proved to be unfounded, since the cooling performance has improved slightly with the longer lines. 100 feet of the total is plumbed with ¼ inch malleable copper tubing.

We have gained considerable experience running a CCD cryostat with the CT cryocooler for extended periods of time. In early operations we could only run continuously for several months at a time before experiencing cooling problems. The CT compressor would sometimes shut off, and this was found to be due to contamination of the gas lines. Recharging the lines and bathing the connectors in helium when they are disconnected or reconnected has eliminated this problem. We have also installed a custom 2 L s^{-1} noble-diode ion pump (from Varian) on the cryostat, and we run the ion pump and vacuum gauge only during the day due to their light emissions. With this setup the system has now been closed for 7 months with little degradation of the vacuum, which is typically $3x10^{-7}$ mbar. We now pump the system approximately twice a year, dictated by occasional warm-ups for HET engineering activities.

The quality of the data has also been improved by the Version 2 controller. In addition to the reduction in readout noise, the new controller has eliminated a bias depression that occurred previously following regions of high signal levels. This was

Downloaded From: https://www.spiedigitallibrary.org/conference-proceedings-of-spie on 15 Jul 2020
Terms of Use: https://www.spiedigitallibrary.org/terms-of-use

due to analog signal processing deficiencies with the previous controller. Now there is no difference between the overscan region count level for bias frames and full exposure flat field frames. The new controller also supports 18-bit digitization. We use it at 16 bits because this is sufficient to span the full well of the CCD (120,000 electrons) and properly sample the readout noise.

3.1.2 New grisms

There are currently two grisms available: grism 1 is 300 l/mm covering 407 to 1170 nm at a resolving power R~600 with a 1 arcsec wide slit; grism 2 is 600 l/mm covering 426 – 730 nm at R~1300. Grism 1 covers more than one octave of wavelength, and is used with blocking filters GG385 or OG515 depending on which part of the wavelength range is needed. Grism 2 is also used with the GG385 blocking filter since the LRS has sensitivity down to 360 nm.

We have been developing a new first-order grism (grism G3) based on a volume holographic grating (VHG)[21]. The wavelength coverage is 630 to 900 nm at R~2000 in first order. This grating has 700 fringes per mm and is used at a Bragg angle of 11.5 degrees. This angle of incidence (and diffraction) is achieved by sandwiching the grating between two identical prisms of SF57 with AR coated outer faces. This grism is described in more detail in 21.

First commissioning observations with this grism have confirmed its high throughput (figure 5) and have offered the opportunity to test the full wavelength range of the LRS for the first time. Grism G3 has high efficiency in second order as well, so using the B filter as a blocker, we were able to check the image quality of the LRS optics close to their lowest wavelength of 360 nm. Without any refocus, we obtained identical point spread functions for wavelengths between 3727 Å and 1 micron observing both calibration lamps through 0.5 arcsec diameter pinholes and the bright Cat's Eye Planetary Nebula (NGC 6543). These observations confirmed the pan-chromatic image size of 0.35 arcsec FWHM for the LRS spectrograph over the 360 to 1000 nm wavelength range, without refocus.

In order to realize the highest possible resolving power from the LRS we have procured two echelle grisms with nominal blaze angles of 63 degrees. Echelle E1 has 316 l/mm and E2 has 79 l/mm. They are both from Richardson Grating Lab. masters, and are used at a 56.5 degree angle of incidence with the grating surface towards the source so that vignetting is avoided by the light propagating in the prism material until close to the camera. These are probably the largest echelle grisms ever deployed. This also allows the exit face of the prism to steer the wavelength range incident on the detector. Smaller versions of E1 and E2 have been used in DFOSC and EFOSC[22], respectively. To date only E1 has been mounted in the instrument and used with V and I band filters as blockers. Initial observations of NGC 6543 show central wavelengths of 783 and 534 nm for orders 2 and 3, and confirm the predicted wavelength coverage. Resolving power is R~2800 for the 1-arcsec wide slit. Full characterization, including throughput measurements, of these grisms will continue in the fall and we expect to make them available at the end of the year.

3.1.3 The Multi-Object Spectroscopy mode

The Multi-Object Spectroscopy (MOS) unit on the LRS has been described in ref 20. It consists of 13 remotely configurable slitlets each approximately 15 arcsec long and 1.3 arcsec wide on 20 arcsec centers. This unit was preferred for LRS over masks due to the remote location of the LRS and the complexity of carrying sufficient numbers of masks to accommodate the wide range of possible observations in the HET queue at any given time. Software configuration files are created ahead of time and uploaded to the MOS unit at the time of observation. Configuration takes only a few minutes and happens in a background thread so that other setup tasks can be executed. The unit has now been in use for about a year for queue observations. For most of that time we have used pre-images obtained with the LRS to set up MOS configurations. In order to realize the power of this unit, we have now enabled setups directly from astrometry, and have created an IRAF package to allow interactive placement of slitlets, with visual feedback[‡]. . There are three options for generating configurations:

- Obtain a short setup image with LRS, and base the configuration on that image. We have mapped the optical distortion of the LRS back to the HET focal surface and the routine *makemos.cl* automatically detects that the image is from the LRS and applies the appropriate corrections. In order to set up the telescope, a fiducial star is needed as well as the slitlet configuration. We also provide the positions of the slitlets for reference
- Use an image from another telescope that has a square (RA-dec) coordinate system in pixel space. Then the task *modmos.cl* is used to generate an image of the appropriate plate scale and rotation, which is then acted on by *makemos.cl* to generate the configuration file and finding chart. Note that images from the digital sky survey (DSS) plates do not have an orthogonal coordinate system, and cannot be used directly.

[‡] The MOS setup package is available at http://hyperion.as.utexas.edu/hetspeccal/moscal/index.html

Downloaded From: https://www.spiedigitallibrary.org/conference-proceedings-of-spie on 15 Jul 2020
Terms of Use: https://www.spiedigitallibrary.org/terms-of-use

- If accurate astrometry already exists, the task lrsart.cl will take a list of coordinates and magnitudes and create an artificial image with an orthogonal coordinate system, which can then be fed through modmos.cl and makmos.cl.

These tasks are now available for use by all PIs in the preparation of MOS configuration files and standard format finding charts. Following exhaustive tests, we have verified that MOS setups can be accurately made using the position angle encoding of the HET and a single fiducial setup object within the central half of the imaging field area. As a result, MOS setups are no more complicated than setting up a longslit observation: the position angle is set, and the telescope is offset under guider control so that the fiducial object is on the appropriate pixel. These setups can be made with no more overhead than for standard longslit observations.

3.1.4 Current LRS performance

The improvement in HET image quality has unfortunately been offset by the degradation in the HET throughput due to the reflective coatings. With the currently delivered images of ~1.5 arcsec FWHM from the HET, the LRS is giving S/N ratios of about 5 per resolution element on R ~ 21 in 30 minute exposures, using a 2.0 arcsec wide longslit and Grism 1. We expect to gain about one magnitude of sensitivity when the image quality meets specifications (1.0 to 1.5 arcsec) and the throughput increases by a factor of nearly two. Unfortunately, it is still difficult to predict how the image size will degrade due to defocus during a track, so there is great uncertainty in the predictions of S/N ratio, but we have obtained data meeting the above numbers. Exposures much longer than 30 minutes can be compromised by the HET defocus, and we are currently recommending that longer exposures be broken into 20 minute segments so that the telescope can be refocused between exposures.

Figure 1 shows the on-sky throughput of the HET plus LRS as measured on a standard star with a 10.0 arcsec wide slit. The efficiency is expressed as the fraction of photons incident on the atmosphere that are detected by the LRS CCD for an

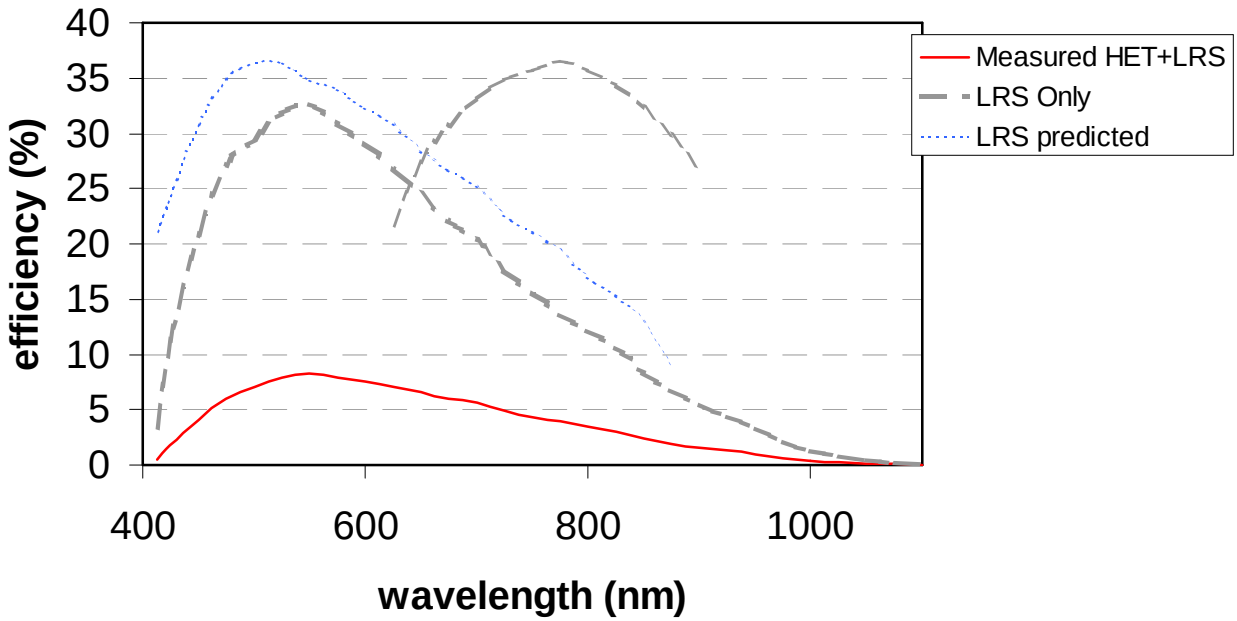

Figure 1. HET and LRS on-sky efficiency measurements. The data were measured with grisms G1 and G3 and the 10.0 arcsec wide slit on standard star HD19445 in March and April 2002. The lower curve is the measured efficiency of HET plus LRS plus atmosphere for a 9.2 m diameter aperture with no obstruction. The heavy dashed curve shows the LRS efficiency after correction for the current performance of the HET (peak throughput about 33%). Grisms G1 and G3 are shown (see text). The light dashed curve is the predicted LRS throughput with G1 from ref 6, for comparison.

unobstructed 9.2 m aperture, and peaks at 8%. Note that equivalent measurements of LRS on-sky efficiency[4] peaked at about 14% for this grism in 1999. That measurement was shown to be consistent with the predictions in ref 6. Since then, the reflective coatings on the primary mirror segments have continued to degrade, and the coatings on two of the four corrector

Downloaded From: https://www.spiedigitallibrary.org/conference-proceedings-of-spie on 15 Jul 2020
Terms of Use: https://www.spiedigitallibrary.org/terms-of-use

mirrors have also degraded significantly (see above). The throughput of the HET at field center inferred from broad band reflectance measurements of the mirrors and the known obstruction factor is now about 33%. It should be 65%. Additionally, in the past several months the coating on the fold-flat that directs light to the LRS has shown visible degradation, accompanied by an estimated loss of a further 30% in throughput. This mirror will be replaced imminently.

3.1.5 LRS science performance

The combination of the image quality delivered by the HET and the degraded reflective coatings make the effective aperture about 7 meters for the LRS. While this is well below the desired performance, it is still a large telescope, and it is very competitive for certain observations. Firstly, for observations where the image quality is irrelevant, the performance rivals other large telescopes. A specific project to measure the dynamics of elliptical galaxies to several effective radii has been very successful[23,24]. The limiting surface brightness for the LRS with the 1 arcsec wide slit and grism 2 (resolving power R~1300) is μ_B = 24.4 mag /Å/sq. arcsec in 1 hour at S/N ratio = 3. Using the Gemini GMOS exposure time calculator, the limit for that instrument is μ_B = 24.0 mag /Å/sq. arcsec, and for the Keck LRIS[25] it is μ_B = 25.0 mag /Å/sq. arcsec at the same S/N and same resolution. The HET LRS beats Gemini GMOS and is competitive with Keck LRIS when the aperture difference is accounted for. The reason for this advantage is that the beam size in the LRS is larger since the instrument was designed to utilize poorer image quality, so the same resolving power is achieved with a larger projected slit width, hence gathering more light. Observations of M86 have reached 3.5 effective radii, the furthest out in any galaxy to date[24]. This performance should improve when the mirrors are re-coated.

HET is very powerful for large surveys, where the sample size can be built up steadily whenever the conditions meet the observing criteria. Using the queue scheduling of the telescope, two large projects have obtained significant samples. More than 100 SDSS QSO and L/T dwarf star candidates have been observed successfully to date[26], with 95% of the observations being of high-enough quality to determine the nature of the object and obtain a redshift. Another large project is the TexOx-1000 radios source redshift survey which aims to measure the evolution of the radio source population with 1000 sources. It is about half complete with half the observations coming from the HET LRS, and is already the largest radio source redshift survey ever[27].

3.2 The High Resolution Spectrograph

The HET High Resolution Spectrograph (HRS) has been described by Tull[9]. It is a fiber-fed, grating cross-dispersed echelle spectrometer that uses Barranne's white-pupil concept as adapted for ESO's VLT UVES by Delabre and Dekker. A refractive camera avoids a central obstruction but limits the bandwidth to 410 nm – 1.05 μm. Details not previously reported are as follows. Light is fed from the HET with either 2 or 3 arcsecond fibers, and the choice of 0, 1, or 2 sky fibers. The 3 fibers of each of the two sizes are in a line and are separated by 10 arcseconds at their input. The output ends of these two fiber sets are mounted on a motorized stage which selects the source to be positioned at the insertion point into the spectrometer. The possible sources are the 2 arcsec fibers, the 3 arcsec fibers, the calibration feed, a prototype fiber image slicer, a black mask, and an unobstructed path to pass a collimation laser. The f/4 light diverging from the output of a source fiber is collimated to a 7.5 mm diameter beam size over a 100 mm length, before being focused at f/10 onto the slit of the spectrometer. The collimated region is used for the filter wheel that suppresses the 2nd order of the cross disperser, for an insertable temperature-stabilized I_2 gas absorption cell, and for an aperture stop at the pupil position which is available when the I_2 cell is retracted. The spectrometer slit mechanism selects one of 12 slits of different widths and lengths that are etched in a metal foil. Resolving powers of 15,000, 30,000, 60,000, and 120,000 are available via a choice of 4 different widths, and the number of sky fibers passed by a given slit is determined by its length. A pinhole that images to 2 CCD pixels (R=120,000) is also on the slit mask. Two cross dispersers are available, each being kinematically mountable at any one of 10 different angles of incidence. The 316 groove mm^{-1} grating gives 400 nm of coverage, with the central wavelength changing in 100 nm steps. The 600 groove mm^{-1} grating gives 200 nm of coverage, with the central wavelength changing in 50 nm steps.

Calibration light does not come down the fibers from the telescope, but rather enters the HRS through a fiber bundle from each of a Th-Ar and flat field lamp outside the HRS enclosure. Within the calibration head on the HRS source selector, the light from the lamp in use diverges out of the fiber bundle over a 20 mm length, passes through a diffuser, and on to an exit slit about 10 mm away. That slit is slightly larger than the widest and longest spectrometer slit, so that all possible spectrometer slits are uniformly illuminated. The aperture stop in the collimated space limits the focal ratio to f/4 to match that of the telescope fibers.

Downloaded From: https://www.spiedigitallibrary.org/conference-proceedings-of-spie on 15 Jul 2020
Terms of Use: https://www.spiedigitallibrary.org/terms-of-use

3.2.1 Observing modes and options

The HRS offers a considerable number of possible configurations, most of which are appropriate for observations of one type or another. For a given observation, an observer specifies the instrument configuration with a string of the following format:

HRS_ResPower_echelle_CrossDisp_fiber_skyfibers_slicer_gascell_binning

e.g. HRS_60k_central_600g5271_3as_1sky_IS0_GC0_2x1

Each token in this string represents a configurable sub-system. There are currently 4 possible resolving powers (ResPower), 3 possible tilts of the echelle grating (echelle), 10 possible tilts of two cross dispersers for 20 possible cross disperser settings (CrossDisp), 2 possible fiber sizes (fiber), 3 possible choices for the number of sky fibers (skyfiber), the choice to use or not use the I_2 gas cell (gascell), and 14 recommended CCD binnings (binning) which depend upon the resolving power. At R=15,000 and R=30,000, the recommended CCD binning corresponds to about 3 pixels per resolution element, at R=60,000 it corresponds to either 2 or 4 pixels per resolution element, and at R=120,000 the only choice is 2 pixels per resolution element. In practice, only a very small number of the many thousands of combinations are used in any one night, making the task of taking calibration frames a practical endeavour.

Full details of the HRS configurations and restrictions are available by following the HRS links from the HET web site at http://het.as.utexas.edu/HET/hetweb/. In particular, order overlap places restrictions on the number of sky fibers that can be used at bluer wavelengths with 316 groove mm^{-1} cross disperser.

3.2.2 CCD system

The CCD system is a mosaic of two Marconi Applied Technologies (now E2V Technologies) 2048 x 4102, 15 micron pixel CCDs. It is called MM1 (Marconi Mosaic #1), and is controlled by a McDonald Observatory Version 2 CCD controller identical to the one described in section 3.1.1 that controls SF1. One amplifier is used per CCD, and they run simultaneously at 100 kpixels per second per amplifier. 18-bit digitization at 0.68 electrons per ADU resolves well the 2.8 electron readout noise while fully spanning the 180,000 electron full well. The CCD controller, with the exception of the preamplifiers and amplifier-related bias supplies, is outside the HRS enclosure so that the 110 W power dissipation of the controller does not disturb the spectrometer. Temperature regulation of the CCD cold mount is approximately 100 μK r.m.s. for excellent stability of the detector system. A CryoTiger cryocooler system is used for cooling the mosaic, and the vacuum is maintained with a 175 cm^3 activated charcoal cryopump, a custom Varian 2 L s^{-1} noble-diode ion pump, and a Pfieffer Full-Range vacuum gauge. The pump and gauge are only run during the day due to their light emissions, and the vacuum is $2x10^{-7}$ mbar or better. The system stays cold typically for six or more months at a time, dictated by occasional warm-ups for HET engineering activities.

The CCDs are oriented such that the columns are parallel to the echelle dispersion dimension, so that the 72-pixel gap between the two CCDs takes out approximately one order rather than the center of all the orders. At R=15,000 and R=30,000, the recommended binning corresponds to about 3 pixels per resolution element, at R=60,000 it corresponds to either 2 or 4 pixels per resolution element, and at R=120,000 the only choice is 2 pixels per resolution element.

The one significant issue is the cosmetic quality of one of the CCDs, MM1-red. While given a grade-1 designation, it has many bright defects, and the charge transfer efficiency is bi-modal depending upon which region of columns is considered.

3.2.3 Current performance

The HRS saw first light in April 2001 and entered routine queue scheduled observing in late May 2001. It has observed objects from 1st to 18th magnitude, at signal-to-noise ratios between 5:1 and 600:1, and at flux levels comparable to the sky flux through the fibers. Very high signal-to-noise ratios have been reported[28] in close agreement with those expected from the detected signal level. The resolution and image shapes across the field from the R=120,000 pinhole are in very close agreement with ray-tracing. The throughput typical of performance in 2001 is given in table 1. It was determined before the decline in the reflectivity of the HET optics, but

Table 1: throughput at the order center for 1800 s integrations in 2" seeing

Resolving power	2 arcsec fibers		3 arcsec fibers	
	V mag.	S/N @ wavelength	V mag.	S/N @ wavelength
15,000			14.0	100 @ 580 nm
30,000	12.1	100 @ 580 nm	12.5	100 @ 580 nm
60,000	10.1	100 @ 580 nm	10.5	100 @ 580 nm
120,000	8.9	100 @ 644 nm	9.3	100 @ 644 nm

Downloaded From: https://www.spiedigitallibrary.org/conference-proceedings-of-spie on 15 Jul 2020
Terms of Use: https://www.spiedigitallibrary.org/terms-of-use

Table 2: Slit transmission as a function of fiber size and resolving power.

Resolving power	Transmission 2-arcsec fiber	Transmission 3-arcsec fiber
15,000	1.000	0.798
30,000	0.624	0.427
60,000	0.323	0.217
120,000	0.163	0.109

also before any of the recent improvements to the HET image quality. Through-put is seen to decline rapidly at the resolving power increases. This is because of the losses given in table 2 due to imaging the output of the fiber on the entrance slit into the HRS. In 1.8 arcsec FWHM seeing, the throughput of the 2 and 3 arcsecond fibers should be the same as the increase in light accepted into the 3 arcsec fiber is negated by the higher slit losses for that fiber. The difference in performance between the two fiber sizes, for a given resolving power, is primarily due to poor acquisition and guiding, to which the 2 arcsec fibers are more susceptible.

The HRS is delivering outstanding radial velocity precision[29] for programs using the I_2 absorption cell at R=60,000. Back-to-back velocity measurements have been taken on a number of stars, and these observation generally agree to within a few tenths of one metre per second. The mean r.m.s. velocity of all the observations of 24 stars for which there is no obvious instability is 3.3 m s^{-1}. Figure 2 shows the measurements for 8 representative stars from that sample. Sources of error include the intrinsic velocity performance of the HRS, the signal-to-noise ratio of the data, intrinsic stellar sources of velocity "jitter", and analysis imperfections. Work is proceeding towards a goal of 1 m s^{-1}.

Figure 2: Examples[29] of radial velocity measurements with HRS

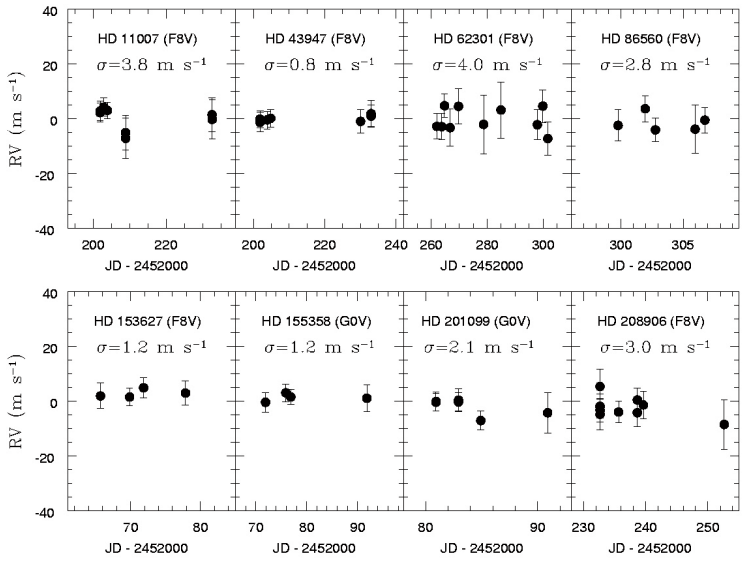

3.2.4 Remaining issues

The HRS is giving excellent data quality and stability, but its competitiveness is significantly reduced by the very poor throughput of the HET/HRS combination. Improvements to the reflectivity of the HET mirrors will improve the telescope throughput by nearly a factor of two. The poor HET image quality requires the use of large fibers to capture a significant fraction of the object flux. Those large fibers are very inefficiently coupled into the available inter-order space of the HRS. The large fibers also capture a large amount of sky flux, brightening the sky-noise limiting magnitude considerably. The improving HET image quality will yield improved coupling both into the fiber at the telescope end, and by use of smaller fibers, improved coupling from the output of the fibers into the HRS.

The most significant issue to be addressed for the HRS is its throughput, and hence its coupling to the HET. Hardware to replace the HET-HRS interface used for commissioning is under design. The key characteristics to improve are these. Acquisition of the object onto the fiber must improve considerable in accuracy and speed to meet specification. Guiding accuracy must come into specification, and telescope focus must be made closed loop to maintain focus within specification. Smaller fibers will be used, probably with 1.5 and 2.0 arcsec diameters, and they will be image sliced. Only one sliced sky fiber will be possible. The collimated space between the output of the fibers and the HRS slit will be increased in length for two reasons. The pupil must always be available for an aperture stop, which is currently not the case when the I_2 absorption cell is inserted, and there will be space for an exposure meter. A two channel exposure meter will give both the object and sky count rate. The spectrometer collimated beam diameter may be reduced for the R=15,000 and 30,000 modes with the two lenses that transfer the fiber output onto the HRS slit. This will allow smaller diameter fibers to be used at these resolving powers where sky brightness is important.

A new calibration source is needed for the HRS to send calibration light down the fibers from the telescope. It is highly desirable that the light pass through the HET corrector and the moving baffle so that the calibration light distribution accurately represents the distribution from the astronomical sources. Additional tasks include improved optical baffling of the HRS, temperature stabilizing the HRS enclosure, and sealing and filtering the air in the enclosure to keep the optics clean.

Downloaded From: https://www.spiedigitallibrary.org/conference-proceedings-of-spie on 15 Jul 2020
Terms of Use: https://www.spiedigitallibrary.org/terms-of-use

3.3 The Medium Resolution Spectrograph

The Medium Resolution Spectrograph is described in references 10 and 11. It provides resolving powers between R=5,000 and 20,000. R~10,000 is an optimal match to a telescope of the HET's aperture and image quality, so we are looking forward to high efficiency with this spectrograph. MRS is a dual-beam fiber-fed grating cross-dispersed echelle instrument. The visible beam (450 – 900 nm coverage) is under going commissioning and the infrared beam (900 – 1300 nm coverage) will be commissioned later. The FIF provides the MRS with multiple fiber-feed options, including 10 multi-object probes, 30-arcsec. fiber longslits, an integral field unit, a sliced fiber for R=20,000, and a scrambled fiber for precision radial velocities. For reference a 2-arcsec diameter fiber gives a resolution of R=5080. The first light spectrum of the daytime sky shows good image quality. A pair of Marconi (now E2V Technologies) 2k x 4k CCDs will provide simultaneous wavelength coverage form 450 to 920 nm with the 316 groove mm^{-1} cross disperser grating. The visible beam of the MRS is expected to deliver S/N ratio ~ 100 in 1 hour at R=5,080 on V=20 stars in 1 arcsec seeing with a 2 arcsec fiber.

4. SUMMARY

The HET has not yet achieved its specified performance in terms of image quality and throughput. Once SAMS is fully operational and the remaining heat sources in the dome are eliminated, we expect the telescope to deliver images approaching the intrinsic site seeing. Slit and fiber insertion losses are currently very significant, even though the HET image quality has improved markedly to about 1.5 arcsec FWHM. The telescope throughput can additionally be doubled by renewing the reflective coatings on the primary corrector mirrors. The LRS and HRS themselves have high throughputs close to predictions, so once the HET throughput is improved, we can expect the instrumentation to perform very well. We also look forward to the MRS entering science operations, which will complete the initial complement of HET facility instruments.

ACKNOWLEDGEMENTS

Special thanks go to John Good, Joe Tufts, Bob Tull, and Marsha Wolf for their contributions to the HET facility instruments described here. We thank the HET operations staff, the McDonald Observatory engineering staff, and particularly Mark Adams, John Booth, Jim Fowler, and Gordon Wesley for their extraordinary efforts in getting HET to its present state of operations. Marcel Bergmann helped with some of the technical achievements discussed in this article.

The Marcario Low Resolution Spectrograph is a joint project of the Hobby - Eberly Telescope partnership and the Instituto de Astronomía de la Universidad Nacional Autónoma de México (IAUNAM). Construction of the HET HRS was funded by NSF Grant AST-9531674, by supplemental funds under NASA Grant NAGW-1477, and by a legislative appropriation from the State of Texas, further supplemented by McDonald Observatory funds.

REFERENCES

1. G. J. Hill, 1995, "Science with the Hobby-Eberly Spectroscopic Survey Telescope," in *Wide Field Spectroscopy*, S.J. Maddox & A. Aragon-Salamanca eds., World Scientific, Singapore, pp. 49-54.
2. J.A. Booth, M.J. Wolf, J.R. Fowler, M.T. Adams, J.M. Good, P.W. Kelton, E.S. Barker, P. Palunas, F.N. Bash, L.W. Ramsey, G.J. Hill, P.J. MacQueen, M.E. Cornell, & E.L. Robinson, "The Hobby-Eberly Telescope Completion Project", in *Large Ground-Based Telescopes*, Proc SPIE **4837**, paper 109, 2002
3. G. J. Hill, "Clustering at High Redshift with the Hobby-Eberly Telescope," in *Clustering at High Redshift*, A. Mazure & O. LeFevre eds., *ASP Conf. Series*, **200**, 226, 2000.
4. G. J. Hill, "The Hobby Eberly Telescope : Instrumentation and Current Performance," in Optical and IR Telescope Instrumentation and Detectors, Proc. SPIE **4008**, 50, 2000.
5. G. J. Hill, P.J. MacQueen, L.W. Ramsey, & E.L. Robinson, 2000, "Early science results from the Hobby – Eberly Telescope," in *Discoveries and Research Prospects from 8-10 Meter-Class Telescopes, Proc. SPIE* **4005**, paper 32.
6. Hill, G. J., Nicklas, H., MacQueen, P. J., Tejada de V., C., Cobos D., F. J., and Mitsch, W., 1998, "The Hobby-Eberly Telescope Low Resolution Spectrograph", in *Optical Astronomical Instrumentation*, S. D'Odorico, Ed., Proc. SPIE **3355**, 375.
7. Hill, G. J., Nicklas, H., MacQueen, P. J., Mitsch, W., Wellem, W., Altmann, W., and Wesley, G. L., 1998, "The Hobby-Eberly Telescope Low Resolution Spectrograph: Mechanical Design", in *Optical Astronomical Instrumentation*, S. D'Odorico, Ed., Proc. SPIE **3355**, 433.
8. F. J. Cobos D, C. Tejada de V., G. J. Hill, and F. Perez G., 1998, "Hobby-Eberly Telescope low resolution spectrograph: optical design," in *Optical Astronomical Instrumentation, Proc. SPIE* **3355**, 424.

Downloaded From: https://www.spiedigitallibrary.org/conference-proceedings-of-spie on 15 Jul 2020
Terms of Use: https://www.spiedigitallibrary.org/terms-of-use

9. R. G. Tull, 1998, "High-resolution fiber-coupled spectrograph of the Hobby-Eberly Telescope," in *Optical Astronomical Instrumentation*, *Proc. SPIE* **3355**, 387.
10. S. D. Horner and L. W. Ramsey, 1998, "Hobby Eberly Telescope medium-resolution spectrograph and fiber instrument feed," in *Optical Astronomical Instrumentation*, *Proc. SPIE* **3355**, 399.
11. L.W. Ramsey, L.G. Engel, N. Sessions, C. de Filippo, M. Graver, "Medium Resolution Spectrograph for the Hobby-Eberly Telescope; Early Commissioning Results", in Instrument Design and Performance for Optical/Infrared Ground-Based Telescopes, *Proc SPIE* **4841**, paper 112, 2002
12. R. K. Jungquist, 1999, "Optical design of the Hobby-Eberly Telescope four-mirror spherical aberration corrector," in *Current Developments in Optical Design and Optical Engineering*, *Proc. SPIE* **3779**, 2.
13. V.L. Krabbendam, T.A. Sebring, F.B. Ray & J.R. Fowler, 1998, "Development and performance of Hobby-Eberly Telescope 11-m segmented mirror," in *Advanced Technology Optical/IR Telescopes VI*, *Proc. SPIE* **3352**, 436.
14. J. A. Booth, F. B. Ray, and D. S. Porter, 1998, "Development of a star tracker for the Hobby Eberly Telescope", in *Telescope Control Systems III*, *Proc. SPIE* **3351**, 298.
15. E.S. Barker, M.T. Adams, F. Deglman, V. Riley, T. George, J.A. Booth, A. Rest, & E.L. Robinson, "Determination of the Intrinsic Ste Seeing for the Hobby-Eberly Telescope" in *Large Ground-Based Telescopes*, Proc SPIE **4837**, paper 25, 2002
16. M.J. Wolf, M. Ward, J.A. Booth, B. Roman, "Polarization shearing laser interferometer for aligning segmented telescope mirrors," in, *Large Ground-Based Telescopes*, *Proc SPIE* **4837**, paper 88, 2002
17. M.J. Wolf, M. Ward, J.A. Booth, A. Wirth, G.L. Wesley, D. O'Donoghue, & L. Ramsey, "Mirror Alignment Recovery System on the Hobby-Eberly Telescope", in *Large Ground-Based Telescopes*, Proc SPIE **4837**, paper 82, 2002
18. M.T. Adams, P. Palunas, J.A. Booth, J.R. Fowler, M.J. Wolf, G. Ames, J. Rakoczy, & E.E. Montgomery, "Hobby-Eberly Telescope Segment Alignment Maintenance System", in *Large Ground-Based Telescopes*, Proc SPIE **4837**, paper 80, 2002
19. J.M. Good, P.W. Kelton, J.A. Booth, E.S. Barker, "Hobby-Eberly Telescope Natural Ventilation System Upgrade", in *Large Ground-Based Telescopes*, Proc SPIE **4837**, paper 26, 2002
20. M.J. Wolf, G.J. Hill, W. Mitsch, F.V. Hessmann, W. Altmann, and K.L. Thompson, 2000, "Multi-object Spectroscopy on the Hobby-Eberly Telescope Low Resolution Spectrograph," in *Optical and IR Telescope Instrumentation and Detectors*, *Proc. SPIE* **4008**, 216, 2000
21. G.J. Hill, M.J. Wolf, J.R. Tufts, & E.C. Smith, "Volume Phase Holographic (VPH) Grisms for Optical and Infrared Spectrographs", in *Specialized Optical Developments in Astronomy*, Proc. SPIE **4842**, paper 05, 2002.
22. H. Dekker, S. D'Odorico, & R. Arsenault, "First Results with a transmission echelle grating on the ESO Faint Object Spectrograph: observations of the SN 1986a and NGC 3367 and the nucleus of the galaxy", Astronomy and Astrophysics, **189**, 353, 1988.
23. K. Gebhardt, "Galactic Nuclei with Large Telescopes", in *Discoveries and Research Prospects from 6- to 10-Meter-Class Telescopes II*, *Proc. SPIE* **4834**, paper 01, 2002.
24. M. Bergmann, "Kinematics and Stellar Populations in the Halo of M86", AAS, **199**, 153.05, 2001; M. Mergmann, K. Gebhardt, & I. Jorgensen, ApJ, in prep., 2003
25. D.D. Kelson, A.I. Zabludoff, K.A. Williams, S.C. Trager, J.S. Mulchaey, & M. Bolte, "Determination of the Dark Matter Profile of Abell 2199 from Integrated Starlight", ApJ, in press, 2002 (astro-ph/0205316)
26. D.P. Schneider, G.J. Hill, X. Fan, L.W. Ramsey, P.J. MacQueen, D.W. Weedman, J.A. Booth, M. Eracleus, J.E. Gunn, R.H. Lupton, M.T. Adams, S. Bastian, R. Bender, E. Berman, J. Brinkmann, I. Csabai, G. Federwitz, V. Gurbani, G.S. Hennessy, G.M. Hill, R.B. Hindsley, Z. Ivezic, G.R. Knapp, D.Q. Lamb, C. Lindenmeyer, P. Mantsch, C. Nance, T. Nash, J.R. Pier, R. Rechenmacher, B. Rhoads, C.H. Rivetta, E.L. Robinson, B. Roman, G. Sergey, M. Shetrone, C. Stoughton, M.A. Strauss, G.P Szokoly, D.L. Tucker, G. Wesley, J. Willick, P.Worthington, and D.G. York, "The Low Resolution Spectrograph of the Hobby-Eberly telescope II. Observations of Quasar Candidates from the Sloan Digital Sky Survey," *PASP*, **189**, 353, 2000.
27. G.J. Hill, J.R. Tufts, M. Bergmann, S. Rawlings, & K. Brand, "TOOT Survey and the Largest Structure in the Universe", in *Discoveries and Research Prospects from 6- to 10-Meter-Class Telescopes II*, Proc. SPIE **4834**, paper 47, 2002.
28. Allende Prieto, C., Lambert, D.L., Tull, R.G., and MacQueen, P.J., "Convective wavelength shifts in the spectra of late-type stars", 2002, ApJ, **566**, L93.
29. W.D. Cochran, R.G. Tull, P.J. MacQueen, D.B. Paulson, M. Endl, A.P. Hatzes, "Searching for ExtraSolar Planets with the Hobby-Eberly Telescope", in *Scientific Frontiers in Research on Extrasolar Planets*, D. Demung, Ed., ASP Conf. Proc., in press.

Downloaded From: https://www.spiedigitallibrary.org/conference-proceedings-of-spie on 15 Jul 2020
Terms of Use: https://www.spiedigitallibrary.org/terms-of-use